Published in final edited form as:
J Mol Cell Cardiol. 2014 December ; 77: 1–10. doi:10.1016/j.yjmcc.2014.09.008.

Stochasticity intrinsic to coupled-clock mechanisms underlies beat-to-beat variability of spontaneous action potential firing in sinoatrial node pacemaker cells:

Unified regulation of sinoatrial node pacemaker cell beating rate and rhythm

Yael Yaniv[1,2,*], **Alexey E. Lyashkov**[3], **Syevda Sirenko**[1], **Yosuke Okamoto**[1], **Toni-Rose Guiriba**[1], **Bruce D. Ziman**[1], **Christopher H. Morrell**[1,4], and **Edward G. Lakatta**[1,*]

[1]Laboratory of Cardiovascular Science, Biomedical Research Center, Intramural Research Program, National Institute on Aging, NIH, Baltimore, Maryland, USA

[2]Biomedical Engineering Faculty, Technion-IIT, Haifa, Israel

[3]Translational Gerontology Branch, Biomedical Research Center, Intramural Research Program, National Institute on Aging, NIH, Baltimore, Maryland, USA

[4]Matematics and Statistics Department, Loyola University, Baltimore, Maryland, USA

Abstract

Recent evidence indicates that the spontaneous action potential (AP) of isolated sinoatrial node cells (SANC) is regulated by a system of stochastic mechanisms embodied within two clocks: ryanodine receptors of the "Ca^{2+} clock" within the sarcoplasmic reticulum, spontaneously activate during diastole and discharge local Ca^{2+} releases (LCRs) beneath the cell surface membrane; clock crosstalk occurs as LCRs activate an inward Na^+/Ca^{2+} exchanger current (I_{NCX}), which together with I_f and decay of K^+ channels prompts the "M clock," the ensemble of sarcolemmal-electrogenic molecules, to generate APs. Prolongation of the average LCR period accompanies prolongation of the average AP beating interval (BI). Moreover, prolongation of the average AP BI accompanies increased AP BI variability. We hypothesized that both the average AP BI and AP BI variability are dependent upon stochasticity of clock mechanisms reported by the variability of LCR period.

We perturbed the coupled-clock system by directly inhibiting the M clock by ivabradine (IVA) or the Ca^{2+} clock by cyclopiazonic acid (CPA). When either clock is perturbed by IVA (3, 10 and 30μM), which has no direct effect on Ca^{2+} cycling, or CPA (0.5 and 5μM), which has no direct effect on the M clock ion channels, the clock system failed to achieve the basal AP BI and both

[*]Corresponding authors: Yael Yaniv, PhD, Biomedical Engineering Faculty, Technion-IIT, Haifa, Israel, yaely@bm.technion.ac.il. Edward G. Lakatta, MD, Laboratory of Cardiovascular Science, Biomedical Research Center, Intramural Research, Program, National Institute on Aging, NIH, Baltimore, Maryland, USA, lakattae@grc.nia.nih.gov.

Disclosures

None.

AP BI and AP BI variability increased. The changes in average LCR period and its variability in response to perturbations of the coupled-clock system were correlated with changes in AP beating interval and AP beating interval variability. We conclude that the stochasticity within the coupled-clock system affects and is affected by the AP BI firing rate and rhythm via modulation of the effectiveness of clock coupling.

Keywords

Ca^{2+} cycling; ion channels; physiology; sarcoplasmic reticulum; sinoatrial nodal pacemaker cells

1. Introduction

The spontaneous action potential (AP) beating interval (BI) of single isolated sinoatrial node cells (SANC) under basal conditions is neither strictly stationary nor completely random, and continuously shifts from one period to another [1–4]. In fact, there is evidence that pacemaker mechanisms intrinsic to SANC play a role in heart rate variability (HRV) (reviewed in [5]), a reduction of which is associated with an increase in morbidity and mortality in patients with cardiac diseases [6]. It has been suggested that AP beating interval variability (BIV) is attributed to stochastic properties of ion channels, components of the M clock [3].

Recent evidence indicates that the average AP BI of isolated SANC is regulated by a coupled-clock system [7]: during diastolic depolarization, a "Ca^{2+} clock" within the sarcoplasmic reticulum (SR) discharges local Ca^{2+} releases (LCRs) close to the cell surface membrane that activate the Na^+/Ca^{2+} exchanger. Na^+-Ca^{2+} exchange current, the f-channel current, and K^+ channel current, other members of the ensemble of sarcolemmal electrogenic molecules ("M clock"), concurrently drive the diastolic membrane depolarization to ignite the next AP. The occurrence of an AP synchronizes global ryanodine receptor (RyR) activation. Spontaneous local RyR activation begins to occur during the following diastolic depolarization. LCR periods (i.e., the times of LCR occurrences following the prior AP) are variable, but on average are roughly periodic [8, 9]. Spontaneous local RyR activity that generates LCRs is regulated by both the level of Ca^{2+} cycling, and by the phosphorylation states of proteins that drive biophysical mechanisms that couple the pacemaker cells' M and Ca^{2+} clocks (reviewed in [10]). Among such proteins are SR (phospholamban (PLB) and ryanodine receptors) and M clock proteins (L type and K^+ channels). The protein phosphorylation level is regulated by Ca^{2+} activation of calmodulin-adenylyl cyclase (AC)-dependent protein kinase A (PKA) and Ca^{2+}/calmodulin-dependent protein kinase II (CaMKII).

A reduction in basal intracellular Ca^{2+} or in the activity of Ca^{2+}-dependent phosphorylation mechanisms decreases spontaneous RyR activation, leading to a lower ensemble LCR Ca^{2+} signal that occurs later during diastole [11]. Based on the coupled-clock theory the net result of this reduction in LCR Ca^{2+} signal is less effective activation of NCX and other M clock proteins that are modulated by Ca^{2+}. It has been demonstrated that the average LCR period of the coupled-clock system is related to the average AP BI [12]. Other studies have shown that when the average AP BI becomes prolonged, the AP BIV increases [1]. We

hypothesized that both the average AP BI and AP BI variability are dependent upon stochasticity of clock mechanisms reported by the variability of LCR period.

To unravel clock-crosstalk effects on AP BI and AP BIV, we perturbed clock function by directly inhibiting either the M or Ca^{2+} clock, confirming that the other clock was not **directly** inhibited, and measured AP BIV and LCR period variability as well as the average AP BI and LCR period. To inhibit the M clock, we employed a range of concentrations of ivabradine (IVA), an I_f inhibitor, and to inhibit the Ca^{2+} clock, we employed a range of concentrations of cyclopiazonic acid (CPA), a SR Ca^{2+} pump inhibitor. Our results revealed that inhibition of either clock produces a similar increase in AP BI, AP BIV, and LCR period and LCR period variability. This increased variability of LCR periods is correlated with the increased AP BIV. These results indicate that while the M and Ca^{2+} clocks remain coupled in response to either clock perturbation, the perturbed clock system cannot maintain average basal AP BI and LCR period. The increases in average AP BI and LCR period are linked to increases in AP BIV and LCR variability that are due to the effectiveness of clock coupling. Therefore, our results provide new evidence that modulation of the stochasticity inherent to clock mechanisms regulates both pacemaker cell rate and rhythm.

2. Methods

The experimental protocols have been approved by the Animal Care and Use Committee of the National Institutes of Health (protocol #034LCS2013). We superfused single, isolated rabbit SANC with IVA (3, 10 or 30 μM), a direct surface membrane ion channel blocker, or CPA (0.5 or 5 μM), a direct and specific inhibitor of Ca^{2+} pumping by SERCA2. We measured AP BI, AP BIV, cytosolic Ca^{2+}, SR Ca^{2+} load and LCR characteristics during diastolic depolarization in spontaneously beating SANC. To prove that IVA or CPA directly affects only the M or Ca^{2+} clock, respectively, we measured I_f and $I_{Ca,L}$ in voltage-clamped SANC in response to a high concentration of CPA and measured LCR characteristics in permeabilized SANC in response to IVA. A detailed description of the experimental methods is available in the Online Data Supplement.

3. Results

3.1 IVA directly and selectively affects only the M clock and CPA directly and selectively suppresses the intracellular Ca^{2+}clock

To test the hypotheses that average AP BI, AP BIV, average LCR period and LCR period variability regulate and are regulated by stochasticity within coupled-clock mechanisms, we directly perturbed either the M or Ca^{2+} clock. We then determined the extent to which direct inhibition of each clock affects the coupled-clock mechanism function.

It is essential to demonstrate at the outset that perturbation of a given clock has no **direct** effect on the other clock. We employed IVA to directly perturb the M clock functions. We used 3 different concentrations of IVA: 3 μM, demonstrated previously to selectively inhibit the funny current and no other M clock component [13, 14]; 10 μM, demonstrated previously to directly inhibit both the L-type channels as well as the funny current [13, 14]; and 30 μM, which also inhibits both the funny current and L-type channels and induces the

maximum drug-induced reduction in AP firing rate in SANC [14]. Although the two higher concentrations directly affect only the membrane clock, our goal was to use a drug that directly gradually inhibits only components of the M clock, and not of the Ca^{2+} clock, per se. In order to prove that IVA does not directly suppress Ca^{2+} clock function, we examined the effects of IVA on SR Ca^{2+} cycling by measuring LCR characteristics in permeabilized SANC. IVA did not significantly change LCR frequency (number of LCRs for 100 μm in 1 sec), duration, amplitude and size (Fig. S1). Moreover, neither the Ca^{2+} signal of individual LCRs nor the LCR ensemble Ca^{2+} signal significantly changed in response to any concentration of IVA (Table S1). Because IVA at concentrations from 3 to 30 μM did not significantly affect LCR characteristics (Fig. S1, Table S1), it, therefore, did not have a direct effect to suppress SR Ca^{2+} cycling. Changes in SR Ca^{2+} cycling that accompany a prolongation of the average AP BI induced by IVA are indirect, and occur via clock crosstalk [7].

We employed CPA to directly perturb the Ca^{2+} clock and not directly the M clock. We used 2 different concentrations of CPA: 0.5 μM, demonstrated previously to increase the average AP BI to the same degree as 3 μM IVA [7]; and 5 μM, which induces the maximum increase in AP BI in SANC [15]. We measured the direct effect of CPA on the Ca^{2+} clock by measuring LCR characteristics in permeabilized SANC. In contrast to IVA, both concentrations of CPA significantly changed LCR frequency (number of LCRs for 100 μm in 1 sec), duration, amplitude and size (Fig. S2). Moreover, the Ca^{2+} signal of individual LCRs and the LCR ensemble Ca^{2+} signal significantly changed in response to different concentrations of CPA (Table S1). To prove that CPA directly and selectively inhibits SR Ca^{2+} cycling, and does not directly suppress ion channels crucial to membrane clock function, we examined the effects of 5 μM CPA on $I_{Ca,L}$ and I_f in voltage-clamped SANC. Representative examples of the CPA effect on $I_{Ca,L}$, measured at −5 mV, and the average effect on the I–V relationship of $I_{Ca,L}$ are presented in Figures S3A and S3B, respectively. Average $I_{Ca,L}$ characteristics are listed in Table S2. Peak $I_{Ca,L}$ in voltage-clamped cells, in the presence of 5μM CPA, did not differ from control (−12.9±1 vs −13.1±2 pA/pF, n=8). Moreover, in voltage-clamped SANC, 5μM CPA did not affect peak I_f amplitude or its kinetics (Table S3, Figure S3C–D). Therefore, CPA selectively and directly inhibits SR Ca^{2+} cycling and does not directly affect the M clock. The effect of CPA in prolonging the AP BI is due to clock crosstalk between LCRs and I_{NCX} [7].

3.2 Direct and specific perturbations of the SANC M or Ca^{2+} clock similarly affect spontaneous AP BI

To determine the effect of M clock inhibition (IVA) on AP BI and AP parameters, we superfused single SANC with different concentrations of IVA; each cell was superfused with only one IVA concentration (3, 10, 30 μM) for 10 min. Representative examples of APs and average AP BI are illustrated in Figure 1A–B, respectively. AP parameters in control and in the presence of IVA are summarized in Table S4. On average (n=7 for each concentration) IVA increased the AP BI by 16±2% at 3μM; by 23±4% at 10μM; and by 36±8% at 30μM. In time-control experiments in the absence of drug (n=7), the time-dependent increase in AP BI was only 4±3% (Table S4).

Fig. 1C illustrates the effects of CPA on AP BI in a representative SANC. Fig. 1D shows that, on average (n=7 for each concentration), a direct effect on intracellular Ca^{2+} cycling by CPA was accompanied by an increase in the average spontaneous AP BI (by 18±5% for 0.5μM CPA; by 43±3% for 5μM CPA), i.e., reaching matching AP firing rate reduction effects by low or high IVA concentrations.

3.3 Clock inhibition- induced prolongation of AP BI and an increase in AP BIV

We further investigated whether increases in average AP BI in response to M or Ca^{2+} clock inhibition were accompanied by changes in AP BIV. Figs. 1E–F illustrate representative examples of the beating interval histograms in the presence of an M clock blocker (IVA) or Ca^{2+} clock blocker (CPA), respectively. As the IVA or CPA concentration increases, the beating intervals become more scattered around the mean. Poincaré plots (Fig. 1G–H), in which each beating cycle length is plotted against its predecessor, display the scattering between consecutive AP intervals and depict the magnitude of the AP BIV. M or Ca^{2+} clock blockade increased the scattering pattern of the points within the Poincaré plot compared to control. The increase in scattering around the mean clearly indicates an increase in AP BIV, i.e., a reduction in the extent to which AP BIs are synchronized. This increased AP BIV in response to M or Ca^{2+} clock inhibition is also clearly demonstrated by AP BIV time-domain variability parameters (SDNN, RMSSD, CV, pNN50, Table S5, see on-line supplement for definitions). Note also that the approximate entropy of the beating interval increases as the average AP BI and AP BIV increase (Table S5). Therefore, the increase in AP BI in response to either M or Ca^{2+} clock inhibition is accompanied by an increase in AP BIV.

Fig. 2 illustrates that the relationship of the average AP BI to AP BIV, quantified by coefficient of variation (panel A) or approximate entropy (panel B). The average AP BIV to the average AP BI prior to and in response to different concentrations of either IVA or CPA conforms to similar non-linear parabolic functions. Therefore, the average AP BI and AP BIV are integrated functions of the coupled-clock system and are tightly linked.

3.4 AP BIV and average AP BI are linked to coupled-clock period variability and the average coupled-clock period

To determine if M clock inhibition to prolong the SANC AP BI is accompanied by an indirect effect on intracellular Ca^{2+} cycling, we measured Ca^{2+} in an additional subset of SANC loaded with Fluo 4-AM. Figure 3A illustrates the AP-induced Ca^{2+} transient and spontaneous diastolic LCRs (arrows) in a representative SANC in control. The interval between spontaneous Ca^{2+} transients reports accurately the interval between spontaneous APs that induce these Ca^{2+} transients [16]. Therefore, the interval between Ca^{2+} transient peaks reports the AP BIs [16]. IVA prolonged the average AP BI and AP BIV in this subset of SANC loaded with florescence indicator (Table S6) to a similar extent as in the non-loaded cells (Table S1).

Rate and rhythm of the coupled-clock period—Coupling of the M and Ca^{2+} clock functions determines the average spatial-temporal characteristics of diastolic LCRs [7]. The effects of IVA on LCR characteristics are listed in Table S7. As the IVA concentration increases the LCR size, duration and the average number of LCRs (normalized to 100 μm

cell length and 1-s time interval) become progressively reduced. The LCR period, defined as the time from the peak Ca^{2+} transient (the onset SR Ca^{2+} release triggered by the prior AP) to the LCR onset (as illustrated in Fig. 3A), was progressively prolonged as IVA concentration increased. In the same cell, note that the LCR intervals became significantly more scattered around a prolonged mean as the IVA concentration increased. Note in the representative example that both the distribution of the LCR periods and that of the AP BI shifted to the right as IVA concentration increased (Fig. 3C–D). The distributions of LCR periods around the mean and the distributions of the AP BIs around their mean do not statistically differ (Kolmogorov-Smirnov test of z^2 value; see on-line supplement) in control or in response to different concentrations of IVA. These results indicate that, in conjunction with its effect to prolong the AP BI and increase the AP BIV, M clock inhibition by IVA concomitantly indirectly regulates the Ca^{2+} clock, and the LCR period, a readout of the coupled-clock system function, was prolonged. The number of LCRs recorded under these experimental conditions was less than the minimum needed for statistical analysis of BIV time-domain parameters. However, the increase in LCR period variability is clearly reflected in the Poincaré plots (Fig. 3D). M or Ca^{2+} clock inhibition increased the scattering pattern of the points within the Poincaré plot compared to control. The changes in AP BI scattering (Fig. 3E) in Poincaré plot of cells loaded with fluorescent indicator is similar to that in the non-loaded cells (Fig 1G).

The direct effects of CPA on LCR characteristics were similar to the indirect effect on LCRs in response to IVA (Table S6 and Fig. 4). Note also that the distributions of LCR periods around the mean do not differ from the distributions of the BIs around their mean (Kolmogorov-Smirnov test, see on-line supplement) in control or in response to different concentrations of CPA.

Fig. 5A–D illustrates the average LCR interval and average AP BI histograms in the presence of M clock inhibition (IVA) and Ca^{2+} clock inhibition (CPA) recorded in a group of cells under these protocols. Note also that the distribution of LCR periods around the mean do not differ from the distribution of the BIs around their mean under this protocol. The average AP BIV, quantified by coefficient of variation (panel 5E) or approximate entropy (panel 5F) in control and in response to either different concentrations of IVA or CPA, is correlated with the average LCR period. The relationship of LCR period to AP BI in response to these perturbations (IVA or CPA) conforms to a nonlinear parabolic line (Fig. 5) strictly similar to the relationship between AP BIV and AP BI (Fig. 2)

IVA and CPA effects on the AP-induced Ca^{2+} transient characteristics—Table S6 lists the average characteristics of the AP-induced Ca^{2+} transients prior to and in the present of drugs. Although the peak systolic Ca^{2+} transient (amplitude) and time to peak Ca^{2+} were not significantly altered in conjunction with the prolongation of the spontaneous AP BI in response to IVA, the 90% decay time of intracellular Ca^{2+} ($T\text{-}90_c$) was significantly prolonged. Because $T\text{-}90_c$ is an index of SR Ca^{2+} pumping kinetics [15], which are modulated by the status of PLB phosphorylation, we measured whether the increase in both AP BI and AP BIV in response to IVA at the ser 16 site is accompanied by a reduction in PLB phosphorylation. There was a trend for IVA at 3 μM to reduce the phosphorylation

state at the PLB ser 16 site, which became significantly reduced at concentrations of IVA above 10 μM (Fig. S4).

Direct perturbation of the Ca^{2+} clock by CPA has effects similar to those of IVA on AP-induced Ca^{2+} transients. Specifically, the increase in spontaneous AP BI in response to CPA is accompanied by a prolongation of $T\text{-}90_c$.

3.5 Changes in the rate of SR Ca^{2+} refilling are correlated with AP BI and AP BIV

A prolongation of $T\text{-}90_c$ indicates a reduction in the rate at which the SR refills with Ca^{2+} [15]. Because 1) IVA and CPA both prolong the $T\text{-}90_c$ (Fig. 6), 2) and both IVA and CPA prolong the LCR period and 3) because LCR period is linked to the AP BIV in response to either M or Ca^{2+} clock perturbations, we hypothesized that IVA- and CPA-induced prolongation of the $T\text{-}90_c$ would be correlated with AP BI and AP BIV. Indeed, Fig. 6A–C demonstrates that the AP BI prolongation prior to and in response to either different concentrations of IVA (panel A) or different concentrations of CPA (panel B) is highly correlated with changes in $T\text{-}90_c$. Moreover, the $T\text{-}90_c$ is also correlated with the average coefficient of variation of AP (panel D).

3.6 Changes in SR Ca^{2+} content are correlated with AP BI and AP BIV

Because prolongation of the AP BI by IVA or CPA results in a reduction of Ca^{2+} influx which likely reduces the SR Ca^{2+} content, we tested whether SR Ca^{2+} load is reduced in response to IVA or CPA. To estimate the SR Ca^{2+} content, brief, rapid pulses of caffeine were applied (“spritzed”) onto control cells and cells in the presence of drug (Fig. 7A). IVA, at 3 μM, tended to reduce the peak amplitude of the caffeine-induced Ca^{2+} transient, but only concentrations of IVA above 10 μM significantly reduced it (Fig. S5A). CPA had similar effects as IVA on caffeine-induced Ca^{2+} release (Fig. S5B).

As hypothesized, the prolongation of $T\text{-}90_c$ is highly correlated with a reduction in the SR Ca^{2+} load (Fig. 7B). The AP BIs in control and in response to IVA or CPA are also correlated with changes in SR Ca^{2+} load in response to these drugs (Fig. 7C). Furthermore, changes in average caffeine-induced Ca^{2+} release are also correlated with increases in the coefficient of variation of AP prior to and in response to these drugs (Fig. 7D).

3.7 Coupled-clock function controls $T\text{-}90_c$, LCR period and AP BI

The average $T\text{-}90_c$ prior to and in response to either different concentrations of IVA (Fig. 8A) or CPA (Fig. 8B) is a linear function of the LCR period. The average AP BI prior to and in response to either different concentrations of IVA (Fig. 8C) or different concentrations of CPA (Fig. 8D) is predicted by the concurrent average LCR period. The average LCR period and average AP BI are readouts of the extent to which synchronization of coupled-clock mechanisms exists [7].

4. Discussion

It has been previously shown that an incremental increase in spontaneous AP BI in response to the M clock (IVA) or Ca^{2+}-clock (CPA) inhibition results from changes in crosstalk within the coupled-clock system [7]. The present study extended the range of spontaneous

AP BI prolongation in response to IVA or CPA. The first novel finding of the present study is that stochasticity within the coupled-clock system determines the AP BIV. Because the AP BIV and the average AP BI are highly correlated, the stochasticity of coupled-clock mechanisms is also tightly linked to the average AP BI. Therefore, failure to maintain the basal average AP BI when either M or Ca^{2+} clock function is disturbed reports increased system entropy. Therefore, the complexity of AP BIV goes well beyond autonomic neural input to SANC residing within the sinoatrial node, and SANC response to autonomic receptor stimulation, but also depends on rhythmic mechanisms intrinsic to the pacemaker cells embedded within the sinoatrial node tissue. Specifically, an increase in AP BI in response to suppression of the Ca^{2+} (CPA) or M (IVA) clock markedly increases time-domain variability indices, and markedly increases beating interval entropy (Fig. 1). A similar link between the increase in AP BI and AP BIV in response to acetylcholine has been previously documented [1, 2, 17]. Note, however, that in contrast to IVA or CPA, which has specific direct effects only on the M or the Ca^{2+} clock, respectively, acetylcholine works directly on both [18]. Thus, our results show, for the first time, that by inducing specific inhibition of a single clock, the degree of clock coupling (synchronization of coupled-clock mechanisms) determines not only the AP BI, but also AP BIV. Because direct perturbations of the M or the Ca^{2+} clock lead to similar reductions in AP BI and AP BIV, we may conclude that AP BIV is not determined solely by M clock function, an idea that was previously entertained [4], but also by stochasticity and efficiency of the functions operative within the coupled-clock system.

The second novel, and most important, finding is that changes in LCR period variability are linked to changes in AP BI. Specifically, the pattern of variability in LCR period in response to graded inhibition of either clock is similar to that of AP BIV. Thus, our results demonstrate that the increased variability in AP BI (evoked by selectively perturbing either the M clock or the Ca^{2+} clock) is related to, and inseparable from, the concurrent variability in LCR periodicity. Similar results were documented in isolated rabbit SANC: beat-to-beat variations in the spontaneous AP firing rate under basal conditions are directly correlated with beat-to-beat variations in the LCR period [8]. We interpret the link between LCR period variability and AP BI variability as resulting from inherently stochastic coupled-clock mechanisms: Stochastic openings of ryanodine receptors generate LCRs during the diastolic depolarization phase. The LCR characteristics (e.g., periodicity) depend upon the available Ca^{2+} (“the oscillatory substrate”) for SR Ca^{2+} cycling that is regulated by the balance of Ca^{2+} influx into and efflux from the cell. Therefore, the stochasticity of LCR periods not only depends upon intrinsic RyR stochasticity of spontaneous RyR activation but also upon sarcolemmal ion channel openings and closings that regulate the cell Ca^{2+} balance. Thus, the stochasticity of LCR periods is a function of stochasticity inherent to both M (stochastic process of ion channels opening) and Ca^{2+} clocks (stochastic opening of RyR channels). When the amount of Ca^{2+} available for Ca^{2+} pumping into the SR is reduced (either by reducing Ca^{2+} influx (IVA) or Ca^{2+} pumping rate (CPA)), the SR Ca^{2+} cycling kinetics become reduced, as evidenced by a prolongation of AP-induced Ca^{2+} transient ($T\text{-}90_C$; an index of the rate of SR Ca^{2+} pumping). Not only is the average LCR period prolonged, but the LCR period variability increases. The increase in LCR variability, in turn, results in a peak ensemble LCR Ca^{2+} signal that not only occurs later in diastole but is of lower

amplitude (due to a reduced synchronization of individual LCR periods). This weaker LCR signal to M clock proteins reports less-efficient clock coupling. On average, the activation of I_{NCX} is delayed, and the average AP BI therefore is prolonged. On a beat-to-beat basis, increased variation in LCR Ca^{2+} cycling results in beat-to-beat variation of this less-effectual LCR Ca^{2+} signal, producing beat-to-beat variation in the efficiency of clock coupling and thus an increase in AP BIV.

Several mechanisms are involved in the extent of efficiency to which the M and Ca^{2+} clocks are coupled in response to IVA or CPA. At concentrations that directly inhibit only the M clock channels (i.e., L-type, K^+, and funny current) (Fig. S1), IVA indirectly suppresses the Ca^{2+} clock. At low concentration of IVA (3 μM), IVA selectively inhibits only the I_f of the M clock [7, 14]. Under this condition, the indirect reduction in Ca^{2+} influx is only due to prolongation of AP BI: The increase in AP BI induces a net reduction in Ca^{2+} influx per unit time due to less frequent $I_{Ca,L}$ activation (due to fewer beats per unit time). Reduction in Ca^{2+} influx simultaneously leads to: (1) a reduction in SR Ca^{2+} load due to a reduction in Ca^{2+} available for pumping into the SR; (2) prolongation of the LCR period; (3) a shift in Ca^{2+} activation of I_{NCX} to later during diastolic depolarization; and (4) possible reduction in Ca^{2+}-calmodulin activation of AC-cAMP/PKA and CaMKII signaling axes (for review, see [19]), although this was not measured directly in the present study, and will require documentation in future studies. This reduction in phosphorylation of Ca^{2+} cycling proteins further reduces the net Ca^{2+} influx and SR Ca^{2+} load. At high concentrations of IVA (>10μM), the increase in AP BI together with a reduction in Ca^{2+} influx reduced the Ca^{2+} SR load, and informed a similar feedback as the low IVA concentration to entrain the M clock to further increase the AP BI.

Other sarcolemmal voltage-activated K^+ channels, Ca^{2+}-activated K^+ channels and Na^+ currents inform a similar feedback to entrain the M clock to further increase the AP BI. The contribution of the decay of rapid delayed rectifier current (HERK) to the diastolic depolarization phase and its essential role in maintaining the spontaneous AP firing rate have been demonstrated in mammals (e.g. rabbit [20] [21], guinea pig [22], etc). Moreover, the inactivation rate of other voltage-dependent K^+ channels is an essential component of the diastolic depolarization phase [23]. The increase in AP BI in response to IVA or CPA indirectly induces a net reduction in K^+ efflux per unit time due to less frequent I_K activation (due to fewer beats per unit time). This leads to 1) prolongation of the deactivation time of K^+ channels and therefore indirectly to a reduction of I_{NCX} activation, and 2) a reduction in NaK pump current (which reduces the I_{NCX}). Ca^{2+}-activated K^+ channels are also present in pacemaker-like cells [24]. Thus, in response to the indirect or direct effect on the Ca^{2+} cycling by IVA or CPA, respectively, the Ca^{2+}-activated K^+ channels can be directly suppressed. Finally, although the sarcolemmal Na^+ current is absent in cells from the center of the rabbit sinoatrial node, it is abundant in its periphery [25]. The increase in AP BI in response to IVA or CPA induces a net reduction in Na^+ influx during the AP per unit time, due to less frequent I_{Na} activation (due to lower number beats per unit time). This reduction in Na^+ influx simultaneously leads to 1) a reduction of I_{NCX} activation, and 2) a reduction in NaK pump current, similar to the effects of a reduction in K^+ outflow. Therefore, in this

case, a change in the degree to which coupled-clock mechanisms are synchronized is indirectly affected by changes in the sarcolemmal voltage-activated Na channel current.

In contrast to IVA, at both tested concentrations, CPA directly suppresses only the Ca^{2+} clock and indirectly suppresses the M clock channels. CPA affects neither I_{Ca} nor I_f (Fig. S3). Similarly CPA does not affect I_{Ca} measured in skeletal muscle [26] or in the heart [27]. Moreover, at similar concentrations, CPA does not affect the Ca^{2+}-dependent K^+ currents in guinea pig smooth muscle cells [28]. Similar to the entrainment effect of the increase in AP BI by IVA on the Ca^{2+} clock, the increase in AP BI in response to CPA also involves crosstalk between the M and Ca^{2+} clocks. In both cases (IVA or CPA), the new steady-state equilibrium in AP BI and AP BIV is achieved due to three factors: (1) the balance is achieved between Ca^{2+} efflux via I_{NCX} and the reduced Ca^{2+} influx [29]; (2) the extent to which reduction in AP firing rate allows the I_f to increase (increase the activation) [30] and I_K to decrease; (3) the extent to which a reduction in Ca^{2+} decreases the L-type channel inactivation [31].

Although our paper is focused on how intrinsic properties of single isolated pacemaker cells affect the beating interval and beating interval variability, one cannot exclude the fact that the pacemaker cells reside in the sinoatrial node. Isolation of single cells from the sinoatrial node precludes cell-to-cell interactions within the tissue increasing both intrinsic clock period and the variability of beating intervals in single SANC compared to the sinoatrial node [17]. Pacemaker cells within intact SAN tissue that have the shortest clock periods entrain cells with more prolonged periods, reducing the BIV among cells within the SAN tissue. This “neighborhood” effect within SAN tissue affects the AP BIV by reducing the variability of properties intrinsic to the entrained cells [32].

5. Limitations

A large literature reporting the effects of pharmacological maneuvers and molecular properties of proteins demonstrates that a diversity of cell types is present within SAN (for review, cf [33]). Specifically, primary and peripheral cell types have different distributions of ionic channels although their “Ca^{2+} clock” components are similar [34]. Because IVA and CPA act directly and indirectly on both components of the coupled-clock system, these interventions may indeed have different effects on beating intervals and beating interval variability in different cell types. Unfortunately, the exact in vivo location or function of cells isolated from the SAN, using the tools of the present study, cannot be determined.

6. Summary

While earlier seminal papers, including those of our own lab, provide a substantial understanding of and novel mechanistic insights into sinoatrial node AP firing and how it is regulated by coupled-clock mechanisms, the majority of these papers have focused only on those mechanisms that control the **average** sinoatrial node AP BI. However, how, and to what extent, these intrinsic coupled-clock mechanisms control the beat-to-beat **variability** of AP BI had not been thoroughly investigated. The present study shows that a reduction in the efficacy of clock coupling effected by direct M or Ca^{2+} clock inhibition not only increases the AP BI but also the AP BIV. The most important findings of our study are (1) when the

clock mechanisms become impaired an increase in LCR period variability is linked to the increase in AP BIV, and (2) LCR period variability increases as the average LCR period and AP BI increase. Thus, the pattern of variability in LCR period in response to graded inhibition of either clock is similar to that of AP BIV. Consequently, modulation the stochasticity within the coupled-clock system regulates the entire range of not only physiological AP firing rate but also its rhythms. Finally, our paper, in demonstrating that variability of functions intrinsic to pacemaker cells, provides definitive evidence that the complexity of heart rate variability measured in vivo goes well beyond the autonomic impulses to the SAN and response of pacemaker cells to autonomic receptor stimulation, but also depends upon mechanisms (e.g. phosphorylation mechanisms, opening and closing of ion channels and ryanodine receptors, etc.) intrinsic to the pacemaker cells embedded within the sinoatrial node tissue.

Supplementary Material

Refer to Web version on PubMed Central for supplementary material.

Acknowledgments

Sources of Funding

The work was supported in part by the Intramural Research Program of the National Institute on Aging, National Institutes of Health and by Technion V.P.R Fund – Krbling Biomedical Engineering Research Fund (Y.Y).

We thanks Ms. Ruth Sadler for text editing.

Non-standard abbreviations and acronyms

AC	Adenylyl-cyclases
AP	Action potential
BI	Beating interval
BIV	Beating interval variability
CaMKII	Calmodulin-dependent protein kinase II
CPA	Cyclopiazonic acid
HR	Heart rate
HRV	Heart rate variability
IVA	Ivabradine
LCR	Local Ca^{2+} release
M	Membrane
PKA	Protein kinase A
PLB	Phospholamban
RyR	Ryanodine receptor

SANC	Sinoatrial-node cell
SR	Sarcoplasmic reticulum
T-50$_c$	50% decay time of intracellular Ca^{2+}
T-90$_c$	90% decay time of intracellular Ca^{2+}

References

1. Rocchetti M, Malfatto G, Lombardi F, Zaza A. Role of the input/output relation of sinoatrial myocytes in cholinergic modulation of heart rate variability. Journal of cardiovascular electrophysiology. 2000; 11:522–30. [PubMed: 10826931]
2. Zaza A, Lombardi F. Autonomic indexes based on the analysis of heart rate variability: a view from the sinus node. Cardiovascular research. 2001; 50:434–42. [PubMed: 11376619]
3. Verheijck EE, Wilders R, Joyner RW, Golod DA, Kumar R, Jongsma HJ, et al. Pacemaker synchronization of electrically coupled rabbit sinoatrial node cells. The Journal of general physiology. 1998; 111:95–112. [PubMed: 9417138]
4. Papaioannou VE, Verkerk AO, Amin AS, de Bakker JM. Intracardiac origin of heart rate variability, pacemaker funny current and their possible association with critical illness. Current cardiology reviews. 2013; 9:82–96. [PubMed: 22920474]
5. Yaniv Y, Lyashkov AE, Lakatta EG. The fractal-like complexity of heart rate variability beyond neurotransmitters and autonomic receptors: signaling intrinsic to sinoatrial node pacemaker cells. Cardiovascular Pharmacology: Open Access. 2013; 2:11–4.
6. Reil JC, Robertson M, Ford I, Borer J, Komajda M, Swedberg K, et al. Impact of left bundle branch block on heart rate and its relationship to treatment with ivabradine in chronic heart failure. Eur J Heart Fail. 2013; 15:1044–52. [PubMed: 23696612]
7. Yaniv Y, Sirenko S, Ziman BD, Spurgeon HA, Maltsev VA, Lakatta EG. New evidence for coupled clock regulation of the normal automaticity of sinoatrial nodal pacemaker cells: bradycardic effects of ivabradine are linked to suppression of intracellular Ca(2)(+) cycling. Journal of molecular and cellular cardiology. 2013; 62:80–9. [PubMed: 23651631]
8. Monfredi O, Maltseva LA, Spurgeon HA, Boyett MR, Lakatta EG, Maltsev VA. Beat-to-Beat Variation in Periodicity of Local Calcium Releases Contributes to Intrinsic Variations of Spontaneous Cycle Length in Isolated Single Sinoatrial Node Cells. PLoS One. 2013; 8:e67247. [PubMed: 23826247]
9. Monfredi OJ, Maltseva LA, Boyett MR, Lakatta EG, Maltsev VA. Stochastic Beat-To-Beat Variation in Periodicity of Local Calcium Releases Predicts Intrinsic Cycle Length Variability in Single Sinoatrial Node Cells. Biophysical journal. 2011; 100:558a.
10. Maltsev VA, Lakatta EG. The funny current in the context of the coupled-clock pacemaker cell system. Heart Rhythm. 2013; 9:302–7. [PubMed: 21925132]
11. Stern MD, Maltseva LA, Juhaszova M, Sollott SJ, Lakatta EG, Maltsev VA. Hierarchical clustering of ryanodine receptors enables emergence of a calcium clock in sinoatrial node cells. The Journal of general physiology. 2014; 143:577–604. [PubMed: 24778430]
12. Lakatta EG, Maltsev VA, Vinogradova TM. A coupled SYSTEM of intracellular Ca2+ clocks and surface membrane voltage clocks controls the timekeeping mechanism of the heart's pacemaker. Circulation research. 2010; 106:659–73. [PubMed: 20203315]
13. Yaniv Y, Maltsev VA, Ziman BD, Spurgeon HA, Lakatta EG. The "Funny" Current Inhibition by Ivabradine at Membrane Potentials Encompassing Spontaneous Depolarization in Pacemaker Cells. Molecules. 2012; 17:8241–54. [PubMed: 22777191]
14. Thollon C, Cambarrat C, Vian J, Prost JF, Peglion JL, Vilaine JP. Electrophysiological effects of S 16257, a novel sino-atrial node modulator, on rabbit and guinea-pig cardiac preparations: comparison with UL-FS 49. British journal of pharmacology. 1994; 112:37–42. [PubMed: 8032660]

15. Vinogradova TM, Brochet DX, Sirenko S, Li Y, Spurgeon H, Lakatta EG. Sarcoplasmic reticulum Ca2+ pumping kinetics regulates timing of local Ca2+ releases and spontaneous beating rate of rabbit sinoatrial node pacemaker cells. Circulation research. 2010; 107:767–75. [PubMed: 20651285]
16. Yaniv Y, Stern MD, Lakatta EG, Maltsev VA. Mechanisms of beat-to-beat regulation of cardiac pacemaker cell function by Ca(2)(+) cycling dynamics. Biophysical journal. 2013; 105:1551–61. [PubMed: 24094396]
17. Yaniv Y, Ahmet I, Liu J, Lyashkov AE, Guiriba TR, Okamoto Y, et al. Synchronization of sinoatrial node pacemaker cell clocks and its autonomic modulation impart complexity to heart beating intervals. Heart Rhythm. 2014; 11:1210–9. [PubMed: 24713624]
18. Lyashkov AE, Vinogradova TM, Zahanich I, Li Y, Younes A, Nuss HB, et al. Cholinergic receptor signaling modulates spontaneous firing of sinoatrial nodal cells via integrated effects on PKA-dependent Ca(2+) cycling and I(KACh). Am J Physiol Heart Circ Physiol. 2009; 297:H949–59. [PubMed: 19542482]
19. Mattiazzi A, Mundina-Weilenmann C, Guoxiang C, Vittone L, Kranias E. Role of phospholamban phosphorylation on Thr17 in cardiac physiological and pathological conditions. Cardiovascular research. 2005; 68:366–75. [PubMed: 16226237]
20. Verheijck EE, Wilders R, Bouman LN. Atrio-sinus interaction demonstrated by blockade of the rapid delayed rectifier current. Circulation. 2002; 105:880–5. [PubMed: 11854131]
21. Sato N, Tanaka H, Habuchi Y, Giles WR. Electrophysiological effects of ibutilide on the delayed rectifier K(+) current in rabbit sinoatrial and atrioventricular node cells. Eur J Pharmacol. 2000; 404:281–8. [PubMed: 10996593]
22. Ding WG, Toyoda F, Matsuura H. Blocking action of chromanol 293B on the slow component of delayed rectifier K(+) current in guinea-pig sino-atrial node cells. British journal of pharmacology. 2002; 137:253–62. [PubMed: 12208783]
23. Irisawa H, Brown HF, Giles W. Cardiac pacemaking in the sinoatrial node. Physiological reviews. 1993; 73:197–227. [PubMed: 8380502]
24. Weisbrod D, Peretz A, Ziskind A, Menaker N, Oz S, Barad L, et al. SK4 Ca2+ activated K+ channel is a critical player in cardiac pacemaker derived from human embryonic stem cells. Proceedings of the National Academy of Sciences of the United States of America. 2013; 110:E1685–94. [PubMed: 23589888]
25. Dobrzynski H, Boyett MR, Anderson RH. New insights into pacemaker activity: promoting understanding of sick sinus syndrome. Circulation. 2007; 115:1921–32. [PubMed: 17420362]
26. Meme W, Leoty C. Cyclopiazonic acid and thapsigargin reduce Ca2+ influx in frog skeletal muscle fibres as a result of Ca2+ store depletion. Acta physiologica Scandinavica. 2001; 173:391–9. [PubMed: 11903131]
27. Badaoui A, Huchet-Cadiou C, Leoty C. Effects of cyclopiazonic acid on membrane currents, contraction and intracellular calcium transients in frog heart. Journal of molecular and cellular cardiology. 1995; 27:2495–505. [PubMed: 8596200]
28. Suzuki M, Muraki K, Imaizumi Y, Watanabe M. Cyclopiazonic acid, an inhibitor of the sarcoplasmic reticulum Ca(2+)-pump, reduces Ca(2+)-dependent K+ currents in guinea-pig smooth muscle cells. British journal of pharmacology. 1992; 107:134–40. [PubMed: 1330156]
29. Eisner DA, Trafford AW. What is the purpose of the large sarcolemmal calcium flux on each heartbeat? Am J Physiol Heart Circ Physiol. 2009; 297:H493–4. [PubMed: 19525376]
30. DiFrancesco D. Characterization of single pacemaker channels in cardiac sino-atrial node cells. Nature. 1986; 324:470–3. [PubMed: 2431323]
31. Kohlhardt M, Krause H, Kubler M, Herdey A. Kinetics of inactivation and recovery of the slow inward current in the mammalian ventricular myocardium. Pflugers Archiv : European journal of physiology. 1975; 355:1–17. [PubMed: 1171426]
32. Jalife J. Mutual entrainment and electrical coupling as mechanisms for synchronous firing of rabbit sino-atrial pace-maker cells. The Journal of physiology. 1984; 356:221–43. [PubMed: 6097670]
33. Boyett MR. ‘And the beat goes on.’ The cardiac conduction system: the wiring system of the heart. Experimental physiology. 2009; 94:1035–49. [PubMed: 19592411]

34. Lyashkov AE, Juhaszova M, Dobrzynski H, Vinogradova TM, Maltsev VA, Juhasz O, et al. Calcium cycling protein density and functional importance to automaticity of isolated sinoatrial nodal cells are independent of cell size. Circulation research. 2007; 100:1723–31. [PubMed: 17525366]

Highlights

- Local Ca^{2+} release period reports the stochasticity of coupled-clock mechanisms.
- Heart rate variability is determined by both membrane and Ca^{2+} clock mechanisms.
- Coupled-clock system stochasticity modulates clock coupling effectiveness.

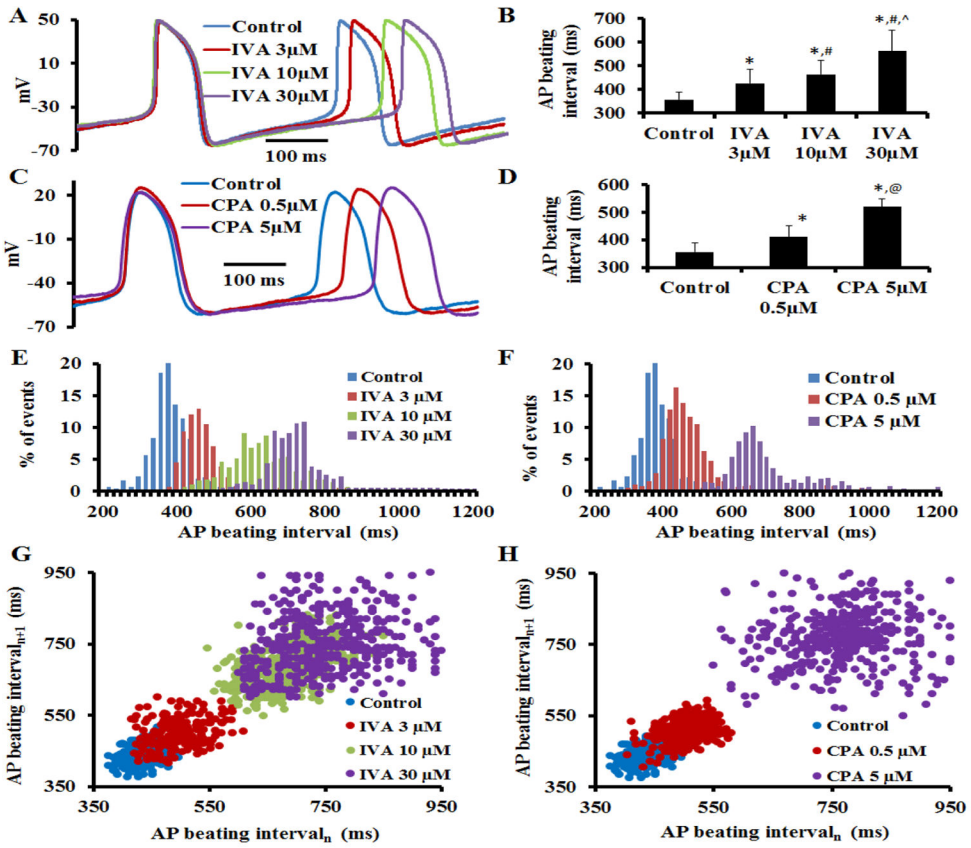

Figure 1. Coupled-clock mechanisms prolongs the spontaneous AP beating interval and increases AP beating interval variability

(A) Representative AP recordings and (B) average changes in the rate of AP firing in the presence of IVA (n=7 for 3, 10 and 30 μM). (C) Representative AP recordings and (D) average changes in the rate of AP firing in the presence of CPA (n=7 for 0.5, 5 μM). Representative distribution of beating intervals in control and in response to (E) IVA or (F) CPA. Poincaré plots of the beating interval in control and in response to (G) IVA or (H) CPA. *p<0.05 vs. control, $^{\#}$p<0.05 vs. IVA 3μM, $^{\wedge}$p<0.05 vs. IVA 10μM, and $^{@}$p<0.05 vs. CPA 5μM.

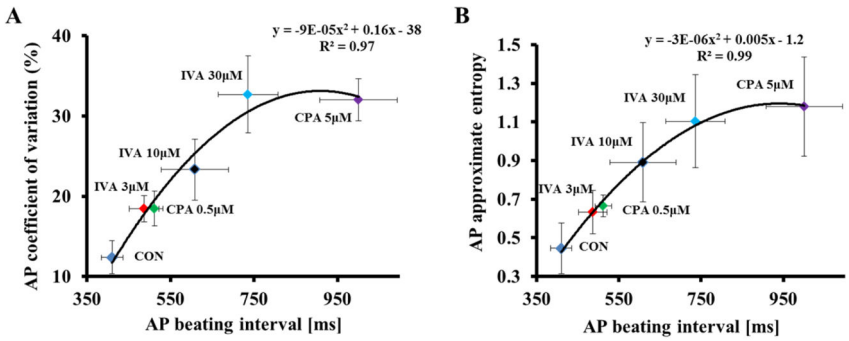

Figure 2. The relationship between changes in spontaneous AP beating interval and AP beating interval variability induced by IVA and CPA

The relationship between average AP BIV quantified by coefficient of variation (A) or approximate entropy (B) to the average AP BI prior to and in response to either different concentrations of IVA or different concentrations of CPA.

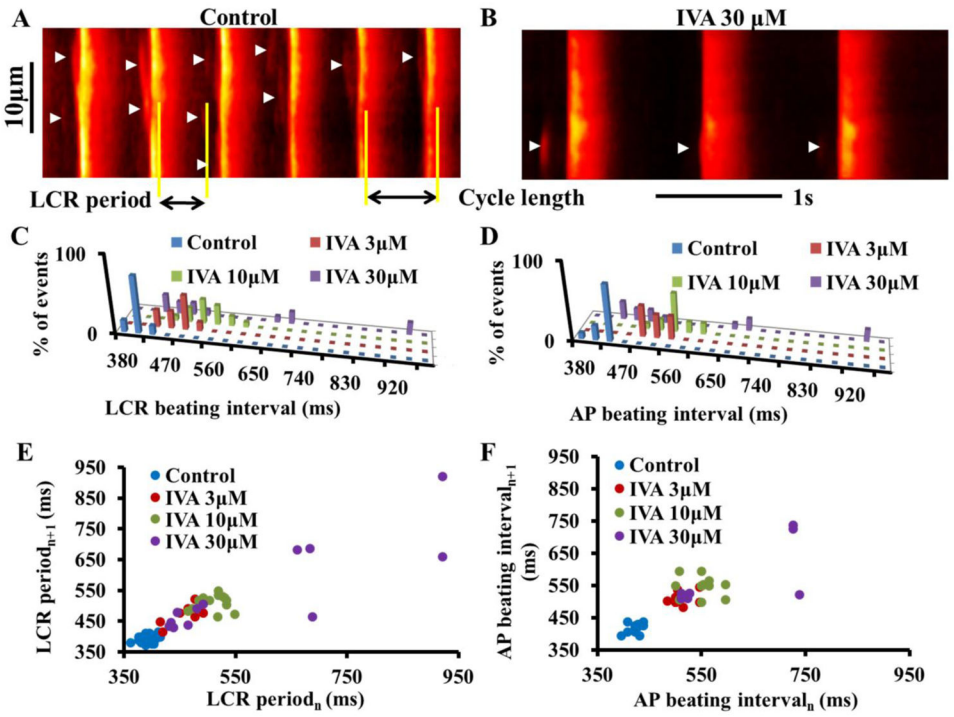

Figure 3. Prolongation of AP beating interval by IVA indirectly affects the LCR period and LCR period variability

Confocal line scan images of Ca^{2+} in a representative SANC (A) in control and (B) in response to 30μM IVA. LCRs are indicated by arrowheads. The LCR period is defined as the time from the peak of the prior AP-induced Ca^{2+} transient to an LCR onset. Distribution of (C) LCR period and (D) AP beating interval in control and in response to IVA in a representative cell. Poincaré plots of (E) the LCR period and (F) the AP beating interval in control and in response to IVA.

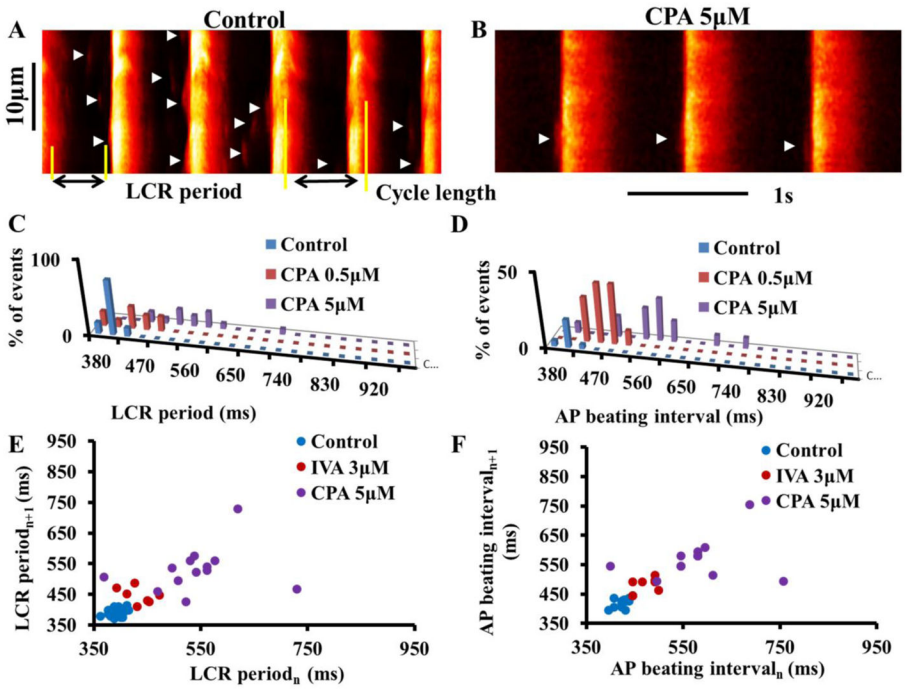

Figure 4. CPA directly affects the LCR period and LCR period variability

Confocal line scan images of Ca^{2+} in a representative SANC (A) in control and (B) in response to 5μM CPA. LCRs are indicated by arrowheads. The LCR period is defined as the time from the peak of the prior AP-induced Ca^{2+} transient to an LCR onset. Distribution of (C) LCR period and (D) AP beating interval in control and in response to CPA in a representative cell. Poincaré plots of (E) the LCR period and (F) the AP beating interval in control and in response to CPA.

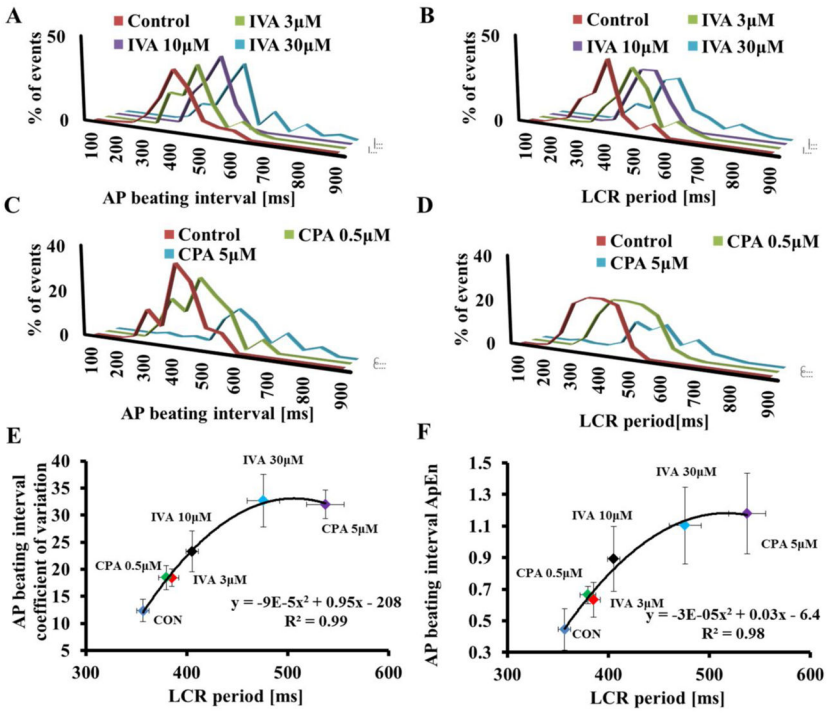

Figure 5. Effect of clock uncoupling by IVA or CPA on LCR period variability

(A) AP-induced Ca^{2+} transient beating interval and (B) LCR period distributions (n=12 cells for each drug concentration, 121, 77 and 65 LCRs for 3, 10 and 30μM IVA, respectively). (C) AP-induced Ca^{2+} transient beating interval and (D) LCR period distribution in control (n=12 cells, 152 LCRs) and the presence of 0.5 μM CPA (n=12 cells, 114 LCRs), or 0.5 μM CPA (n=12 cells, 58 LCRs). The relationship between the average AP BIV, quantified by coefficient of variation (E) or as approximate entropy (F) to the LCR period prior to and in response to different concentrations of either IVA or CPA.

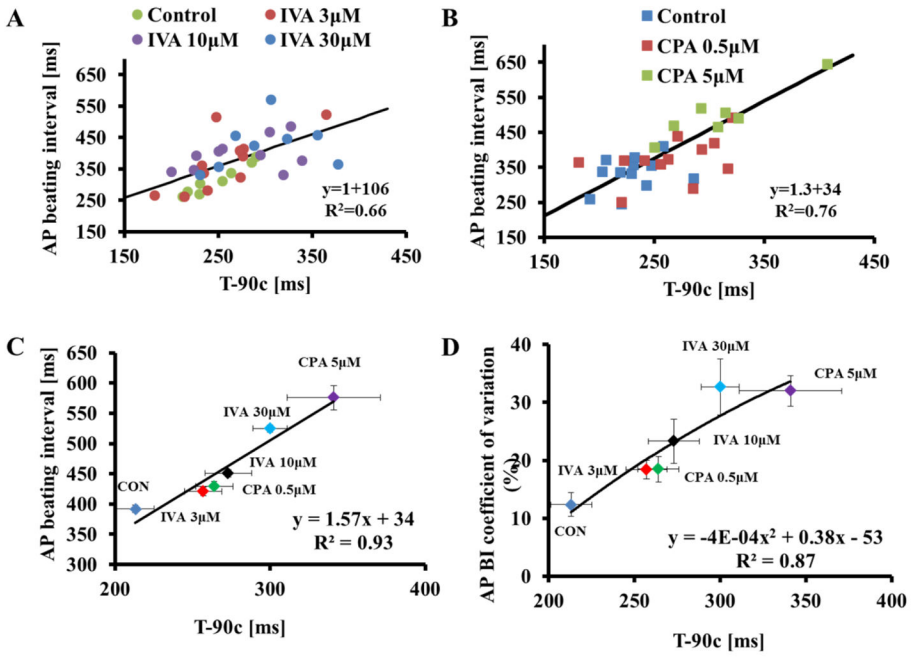

Figure 6. Both CPA and IVA increase the SR Ca^{2+} refilling time

The $T\text{-}90_c$ in control or in the presence of (A) IVA or (B) CPA is correlated with the average AP cycle length. The relationship between (C) average AP beating interval and (D) average AP beating interval variability (quantified by the coefficient of variation) to T-90c prior to and in response to different concentrations of either IVA or CPA.

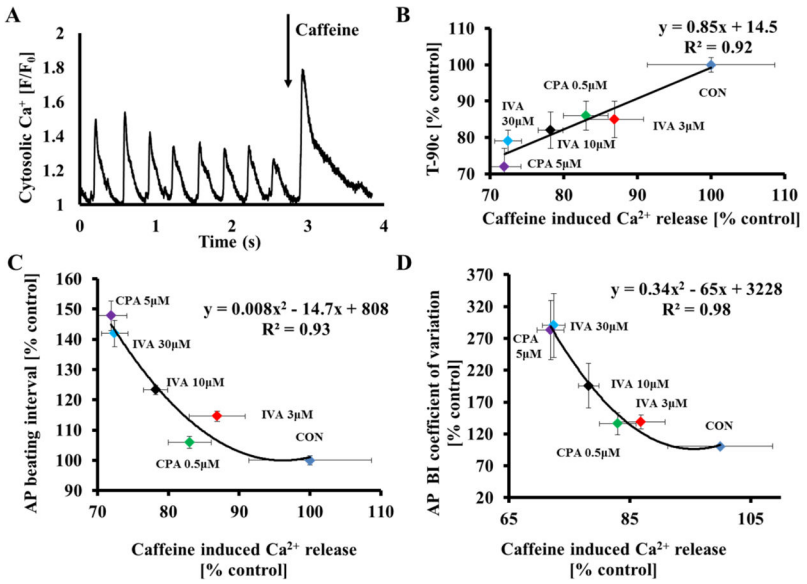

Figure 7. Both CPA and IVA reduce SR Ca^{2+} load

(A) Representative example of the effects of a rapid application of caffeine onto a SANC. (B) The relationship between changes in the average $T\text{-}90_c$ and caffeine-induced Ca^{2+} release. The relationship between (C) average AP beating interval and (D) average AP beating interval variability to caffeine-induced Ca^{2+} release, quantified by coefficient of variation, prior to and in response to different concentrations of either IVA or of CPA.

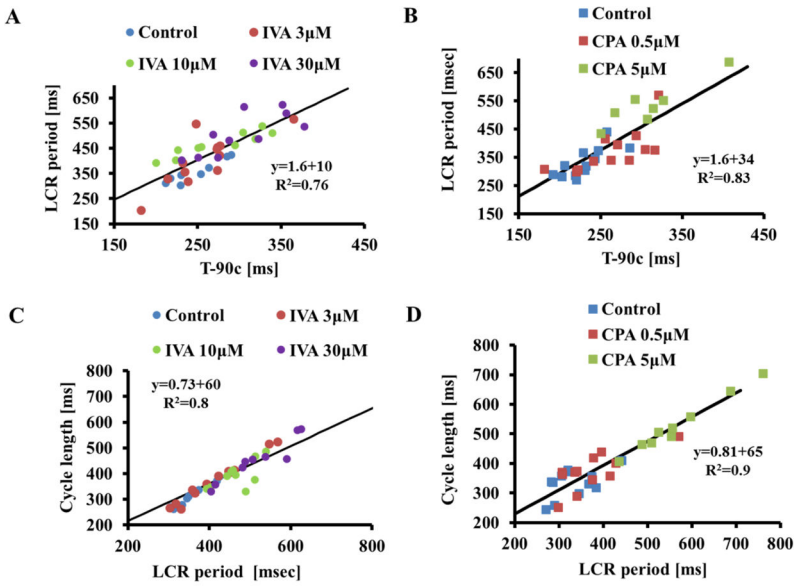

Figure 8. Average AP beating interval and average LCR period are correlated

The LCR period in control or in the presence of IVA (panel A) or CPA (panel B) are correlated with T- 90_c.The LCR period in control or in the presence of IVA (panel C) or CPA (panel D) predicts the concurrent AP cycle length.